Electronic Supplementary Material (ESI) for RSC Advances.

Synthesis and Catalytic Application of *N*-Heterocyclic Carbene Copper Complex Functionalized Conjugated Microporous Polymer

Hui Zhou*, Qing-Yong Zhang and Xiao-Bing Lu*

State Key of Laboratory of Fine Chemicals, Dalian University of Technology, Dalian 116024, China

E-mail:zhouhui@dlut.edu.cn

Table of Contents

1. Characterization of Iodo-NHC-CuCl

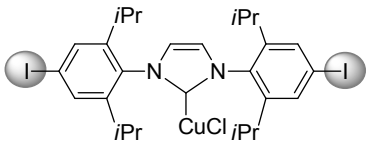

Iodo-NHC-CuCl

^{1}H NMR (400 MHz, $CDCl_3$): δ =7.54 (s, 4H), 7.04 (s, 2H), 2.35–2.42 (m, 4H), 1.21 (d, J = 6.9 Hz, 12H), 1.13 (d, J = 6.9 Hz, 12H). **^{13}C NMR** (100 MHz, $CDCl_3$): δ 147.84, 134.23, 133.98, 123.41, 97.62, 28.87, 24.72, 23.83. **Anal. Calcd** for C27H34N2CuClI2: C, 43.86; H, 4.63; N, 3.79; Found: C, 43.21; H, 4.77; N, 3.35. **HRMS (ESI)**: calcd for C27H34N2CuClI2: 737.9796 [M]. Found: 643.1044 [M-CuCl+H]$^+$.

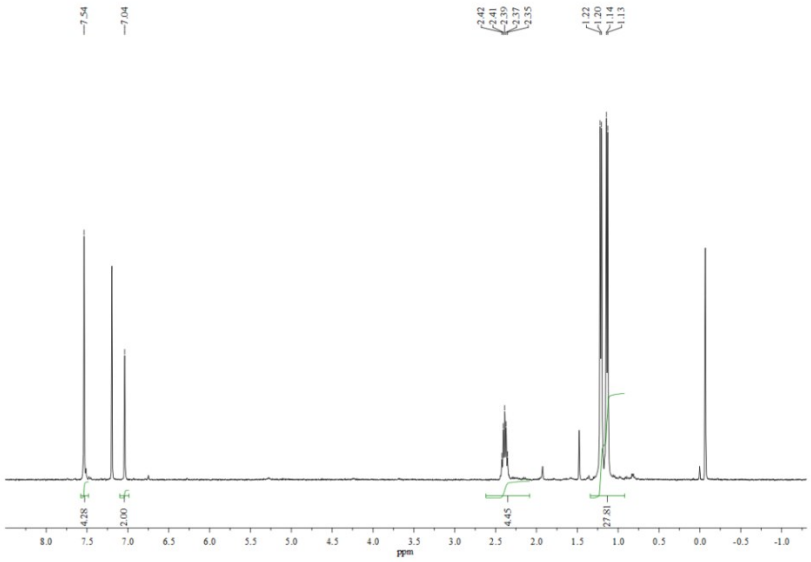

Figure S1. ^{1}H-NMR spectrum of Iodo-NHC-CuCl

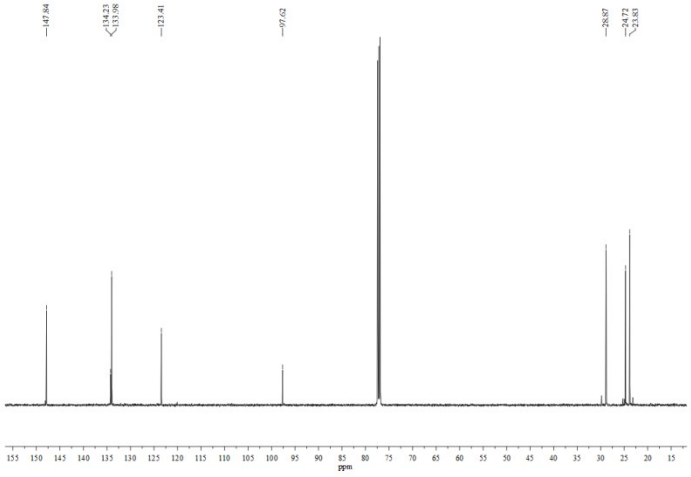

Figure S2. ^{13}C-NMR spectrum of Iodo-NHC-CuCl

2. Characterization of CMP-IPrCuCl

Formation of CMP-IPrCuCl was also confirmed by ^{1}H and ^{13}C cross-polarization magic-angel spinning (CP/MAS) NMR spectroscopy. Based on previous research[1, 2], the resonance peaks at δ= 24.7 (25.8), 56.1, 82.4 (89.7), 128.1, 146.5 ppm (Figure S3) can be assigned to methyl carbon atom **a**, **b**, methenyl carbon atom **c**, acetylenic carbon atoms **d**, **e**, aromatic carbon **f** and imidazolyl carbon atoms **g**, respectively.

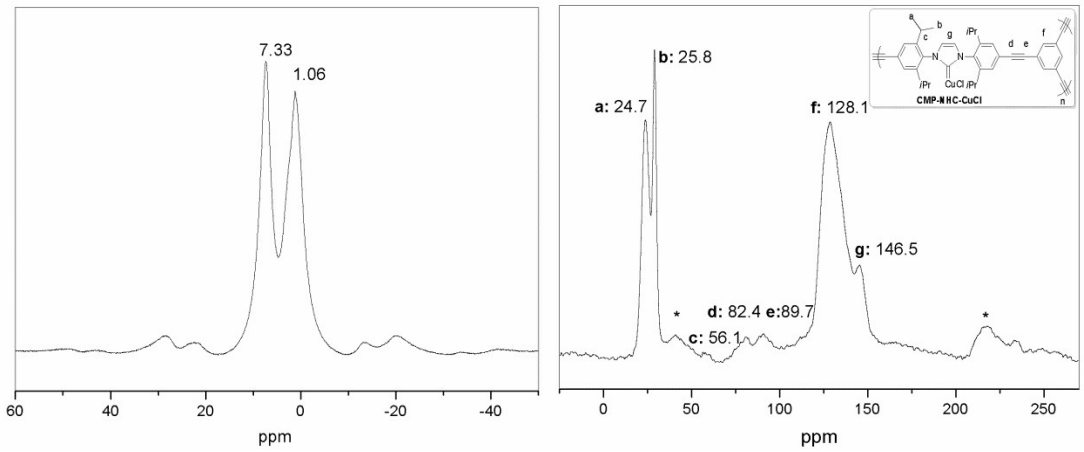

Figure S3. Cross-polarization ^{1}H and ^{13}C MAS NMR spectra of CMP-IPrCuCl in solid state. Asterisk denotes spinning sidebands.

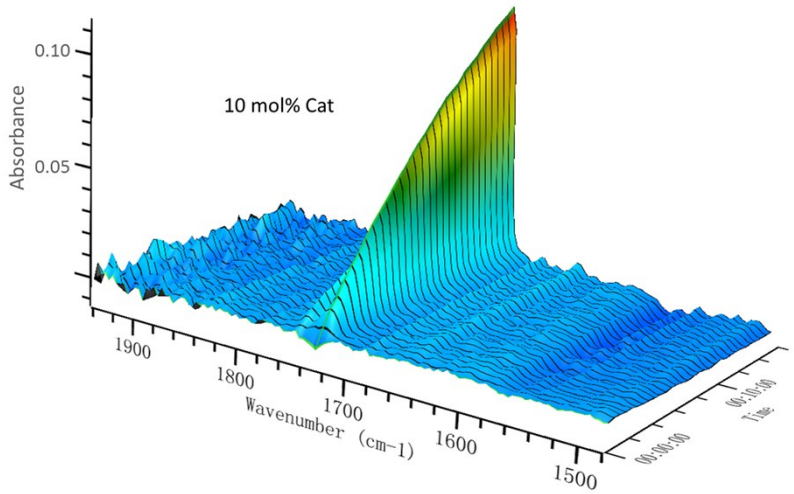

Figure S4. In-Situ monitored hydrosilylation of CO_2 with $(EtO)_3SiH$. (10 mol% Cat.)

3. Kinetic studies.

Under CO_2 atmosphere, a 20 ml flask, equipped with a magnetic stir bar, is charged successively with CMP-IPr(CuCl) (2, 5, 8, 10 mol %, respectively), NaO^{t}Bu (1.2 equiv. to Cat.), $(EtO)_3SiH$ (0.328 g, 2 mmol) and C_6D_6 (1.5 mL), and then In situ FTIR was equipped

to check the IR signals. The absorption peak of 1729 cm^{-1} is assigned to the asymmetric ν(C=O) vibration of the silyl formate. A reaction order of 0.99 of catalyst concentration was obtained from CMP-IPr(CuCl) catalyzed hydrosilylation of CO_2 with $(EtO)_3SiH$ under ambient conditions by altering catalyst concentration, as shown in Figure S4-S5.

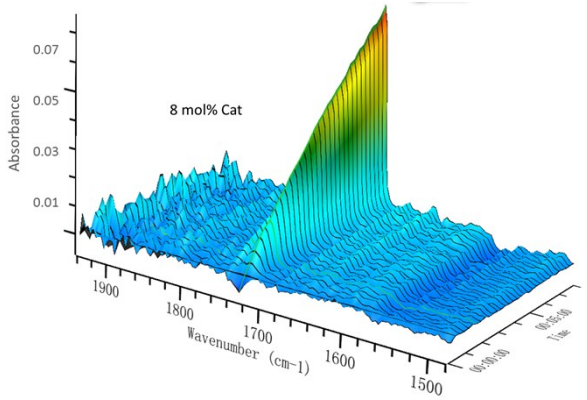

Figure S5. In-Situ monitored hydrosilylation of CO_2 with $(EtO)_3SiH$. (8 mol% Cat.)

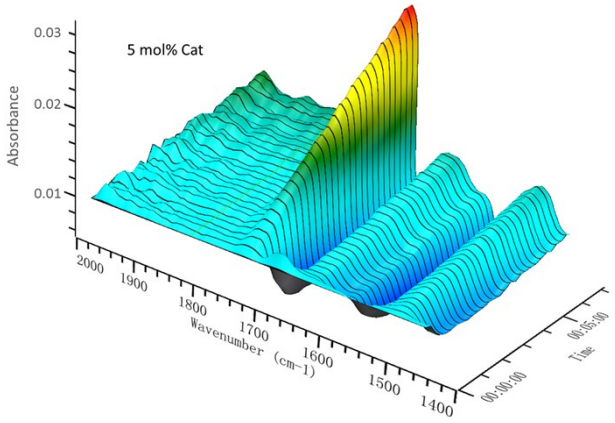

Figure S6. In-Situ monitored hydrosilylation of CO_2 with $(EtO)_3SiH$. (5 mol% Cat.)

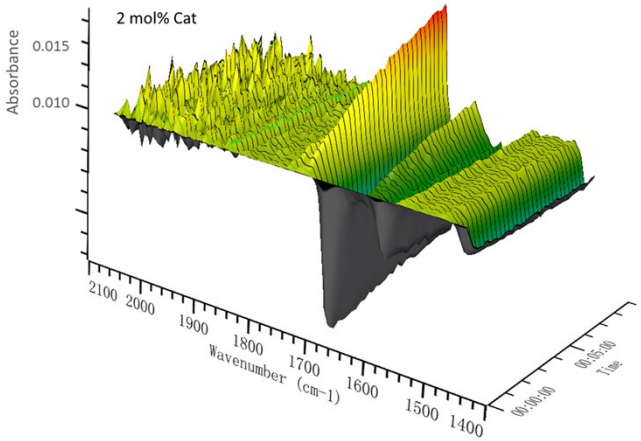

Figure S7. In-Situ monitored hydrosilylation of CO_2 with $(EtO)_3SiH$. (2 mol% Cat.)

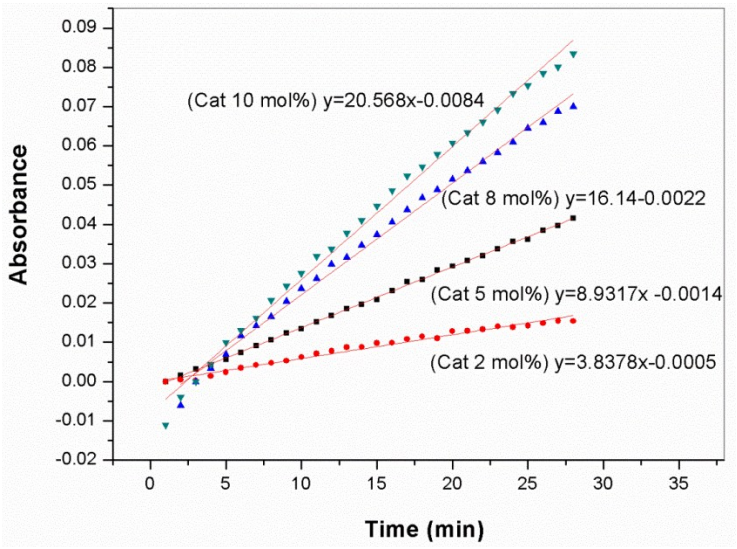

Figure S8. The formation of the silyl formate during the hydrosilylation under different CMP-IPrCuCl concentration.

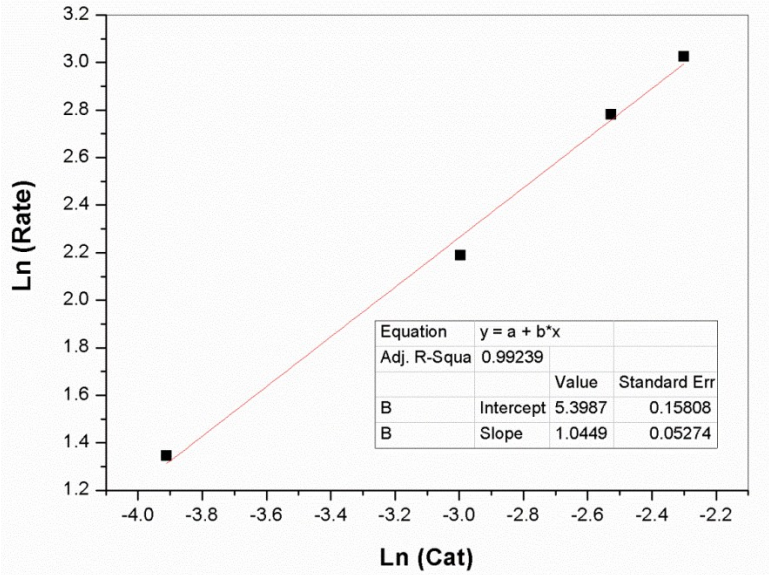

Figure S9. Logarithmic plots of the initial rate of the hydrosilylation of CO_2 with $(EtO)_3SiH$ versus catalyst concentration.

4. Characterization of (β, β)-*E* vinyl disiloxanes (4b-4j).

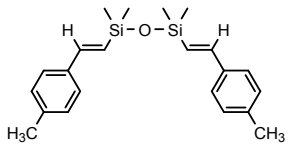

4b ^{1}H NMR (400 MHz, $CDCl_3$): δ 7.34 (d, J = 8.0 Hz, 4H), 7.14 (d, J = 8.0 Hz, 4H), 6.94 (d, J = 19.2 Hz, 2H), 6.39 (d, J = 19.2 Hz, 2H), 2.36 (s, 6H), 0.26 (s, 12H). **^{13}C NMR** (100 MHz, $CDCl_3$): δ 144.53, 138.37, 135.85, 129.54, 127.63, 126.81, 21.58, 1.24.

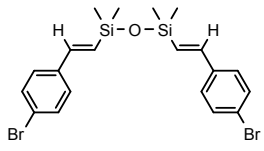

4c ^{1}H NMR (400 MHz, $CDCl_3$): δ 7.44 (d, *J* = 8.4 Hz, 4H), 7.28 (d, *J* = 8.4 Hz, 4H), 6.88 (d, *J* = 19.2 Hz, 2H), 6.42 (d, *J* = 19.2 Hz, 2H), 0.26 (s, 12H). **^{13}C NMR** (100 MHz, $CDCl_3$): δ 143.37, 137.36, 131.98, 129.86, 128.36, 122.41, 1.15.

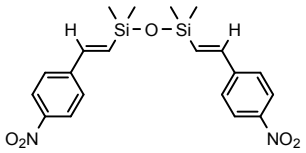

4d ^{1}H NMR (400 MHz, $CDCl_3$): δ 8.18 (d, *J* = 8.8 Hz, 4H), 7.54 (d, *J* = 8.4 Hz, 4H), 7.00 (d, *J* = 19.2 Hz, 2H), 6.64 (d, *J* = 19.2 Hz, 2H), 0.30 (s, 12H). **^{13}C NMR** (100 MHz, $CDCl_3$): δ 147.69, 144.38, 142.32, 134.78, 127.39, 124.33, 1.10.

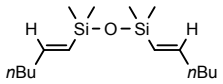

4e ^{1}H NMR (400 MHz, $CDCl_3$): δ 6.07-6.13 (m, 2H), 5.60 (d, *J* = 18.6 Hz, 2H), 2.10-2.12 (m, 4H), 1.31-1.38 (m), 0.90 (t, *J* = 6.4 Hz, 6H), 0.11 (s, 12H). **^{13}C NMR** (100 MHz, $CDCl_3$): δ 148.23, 129.41, 36.35, 30.87, 22.39, 14.12, 0.94.

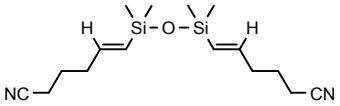

4f ^{1}H NMR (400 MHz, $CDCl_3$): δ 6.01(dt, *J* = 6.2, 18.6 Hz, 2H), 5.70 (d, *J* = 18.6 Hz, 2H), 2.34 (t, *J* = 7.2 Hz, 4H), 2.26 (q, *J* = 6.8 Hz, 4H), 1.74-1.81 (m, 4H), 0.12 (s, 12H). **^{13}C NMR** (100 MHz, $CDCl_3$): δ 144.93, 132.52, 119.82, 35.27, 24.56, 16.76, 1.08.

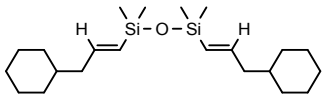

4g ^{1}H NMR (400 MHz, $CDCl_3$): δ 6.06 (dt, *J* = 6.8, 18.6 Hz, 2H), 5.56 (d, *J* = 18.6 Hz, 2H), 2.00 (dt, *J* = 1.0, 6.8 Hz, 4H), 0.84-1.70 (m, 22H), 0.11 (s, 12H). **^{13}C NMR** (100 MHz, $CDCl_3$): δ 147.06, 131.09, 45.23, 37.85, 33.52, 26.93, 26.71, 1.22.

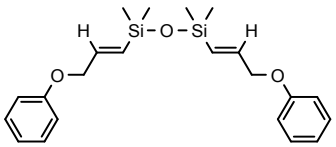

4h ^{1}H NMR (400 MHz, $CDCl_3$): δ 7.25-7.29 (m, 4H), 6.89-6.94 (m, 6H), 6.26 (dt, *J* = 4.4, 18.8 Hz, 2H), 6.00 (d, *J* = 18.8 Hz, 2H), 4.55 (dd, 1.2, 4.4 Hz, 4H), 0.15 (s, 12H). **^{13}C NMR** (100 MHz, $CDCl_3$): δ 158.90, 141.81, 131.95, 129.76, 121.10, 115.02, 70.49, 0.99.

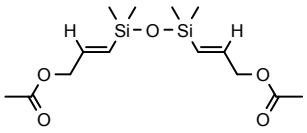

4i ^{1}H NMR (400 MHz, $CDCl_3$): δ 6.11 (dt, *J* = 4.8, 18.8 Hz, 2H), 5.88 (d, *J* = 18.8 Hz, 2H), 4.59 (dd, *J* = 1.0, 4.8 Hz, 4H), 2.09 (s, 6H), 0.14 (s, 12H). **^{13}C NMR** (100 MHz, $CDCl_3$): δ 171.01, 140.49, 132.47, 66.83, 21.30, 0.95.

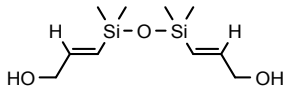

4j **^{1}H NMR** (400 MHz, $CDCl_3$): δ 6.24 (dt, *J* = 4.2, 18.8 Hz, 2H), 5.88 (dt, *J* = 1.8, 18.8 Hz, 2H), 4.18 (dd, *J* = 1.6, 4.2 Hz, 2H), 0.15 (s, 12H). **^{13}C NMR** (100 MHz, $CDCl_3$): δ 145.78, 129.00, 65.40, 0.83.

5. References

1. Rose, M.; Notzon, A.; Heitbaum, M.; Nickerl, G.; Paasch, S.; Brunner, E.; Glorius, F.; Kaskel, S. *Chem. Commun.,* **2011**, *47*, 4814.

2. Xie, Y.; Wang, T.-T.; Liu, X.-H.; Zou, K.; Deng, W.-Q. *Nat. Commun.* **2013**, *4*, 1960.